The α7nACh–NMDA receptor complex is involved in cue-induced reinstatement of nicotine seeking

Shupeng Li,[1] ZhaoXia Li,[1] Lin Pei,[1] Anh D. Le,[1,2] and Fang Liu[1,2]

[1]Department of Neuroscience, Centre for Addiction and Mental Health; and [2]Department of Psychiatry; University of Toronto, Toronto, Ontario M5T 1R8, Canada

Smoking is the leading preventable cause of disease, disability, and premature death. Nicotine, the main psychoactive drug in tobacco, is one of the most heavily used addictive substances, and its continued use is driven through activation of nicotinic acetylcholine receptors (nAChRs). Despite harmful consequences, it is difficult to quit smoking because of its positive effects on mood and cognition that are strong reinforcers contributing to addiction. Furthermore, a formidable challenge for the treatment of nicotine addiction is the high vulnerability to relapse after abstinence. There is no currently available smoking cessation product able to achieve a >20% smoking cessation rate after 52 wk, and there are no medications that directly target the relapse process. We report here that the α7nAChR forms a protein complex with the NMDA glutamate receptor (NMDAR) through a direct protein–protein interaction. Chronic nicotine exposure promotes α7nAChR–NMDAR complex formation. Interestingly, administration of an interfering peptide that disrupts the α7nAChR–NMDAR complex decreased extracellular signal-regulated kinase (ERK) activity and blocked cue-induced reinstatement of nicotine seeking in rat models of relapse, without affecting nicotine self-administration or locomotor activity. Our results may provide a novel therapeutic target for the development of medications for preventing nicotine relapse.

CORRESPONDENCE
Fang Liu:
f.liu.a@utoronto.ca

Abbreviations used: CT, carboxyl tail; ERK, extracellular signal-regulated kinase; GPCR, G protein–coupled receptor; GST, glutathione S-transferase; ICV, intracerebroventricular(ly); IL2, second intracellular loop; nAChR, nicotinic acetylcholine receptor; NMDAR, NMDA glutamate receptor; TAT, transactivator of transcription.

α7 nicotinic acetylcholine receptors (α7nAChRs) and NMDA glutamate receptors (NMDARs) are both ligand-gated ion channels permeable to Ca^{2+} and Na^{+} (MacDermott et al., 1986; Gray et al., 1996). Previous studies have demonstrated modulation of NMDARs by nAChRs, although the molecular mechanism has yet to be identified (Aramakis and Metherate, 1998; Fisher and Dani, 2000; Prendergast et al., 2001; Kenny et al., 2009). Functional regulation of ligand-gated ion channels including the α7nAChR and NMDAR is traditionally thought to be mediated through receptor phosphorylation (Levitan, 1994; Smart, 1997; Swope et al., 1999). However, recent studies have demonstrated that they are also regulated by intracellular proteins and cell surface receptors such as G protein–coupled receptors (GPCRs) through direct protein–protein coupling (Liu et al., 2000; Sheng, 2001; Lee et al., 2002; Kim and Sheng, 2004). To date, functional dimerization of neurotransmitter receptors has been established between GPCRs (Lee et al., 2000; Bulenger et al., 2005; Milligan and Smith, 2007), as well as between GPCRs and ligand-gated ion channels (Liu et al., 2000; Lee et al., 2002). Dimerization between ligand-gated ion channels has not yet been reported. In the current study, we first investigated whether α7nAChR and NMDAR form a protein complex and developed a protein peptide that is able to disrupt this complex. We then determined whether this protein complex was involved in nicotine-seeking behaviors using an operant conditioning-based animal behavioral paradigm: cue-induced reinstatement (Epstein et al., 2006).

RESULTS AND DISCUSSION

To determine the existence of an α7nAChR–NMDAR complex, we tested whether NMDAR coimmunoprecipitates with α7nAChR in rat

The Rockefeller University Press $30.00
J. Exp. Med. 2012 Vol. 209 No. 12 2141-2147
www.jem.org/cgi/doi/10.1084/jem.20121270

The Journal of Experimental Medicine

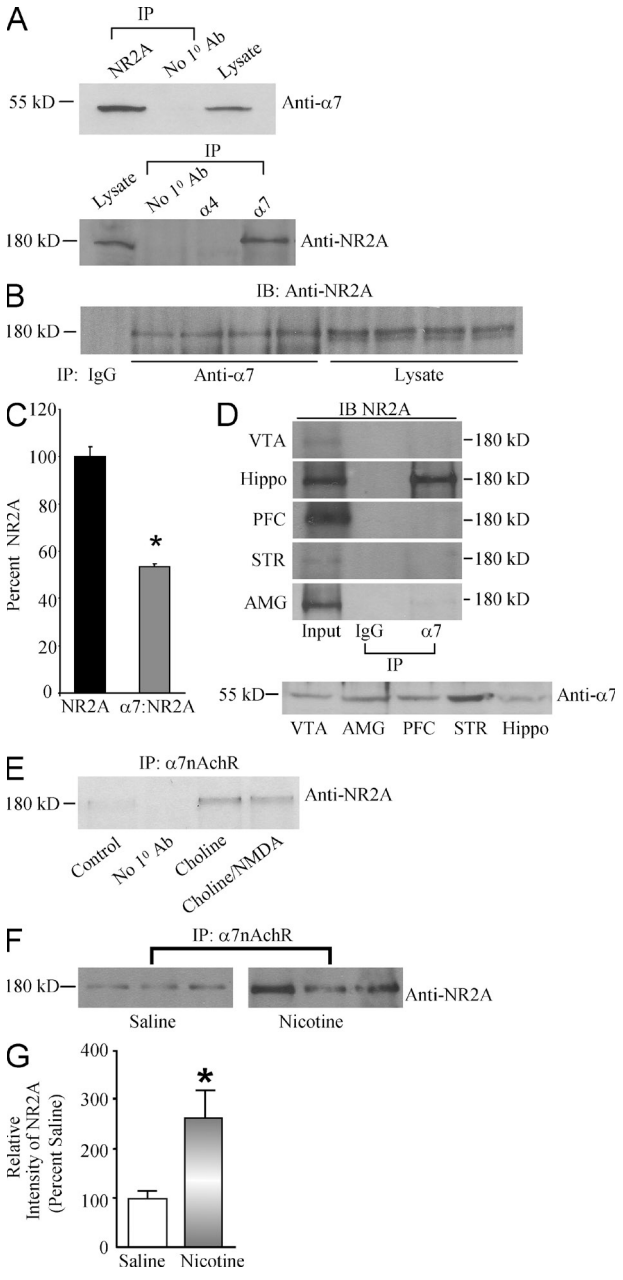

Figure 1. Protein–protein interaction between NMDAR and α7nAChR. (A) Coimmunoprecipitation (IP) of α7nAChR from solubilized rat hippocampal tissue with NR2A subunit (top). Coimmunoprecipitation of NR2A subunit of NMDAR from solubilized rat hippocampal tissue with the α7nAChR but not α4nAChR (bottom). (B) Western blot analysis of the NR2A subunit coimmunoprecipitated by α7nAChR antibody versus the total NR2A in an equal amount of hippocampal protein used in the coimmunoprecipitation experiment. (C) Quantification analysis of Western blots in B by densitometry with ImageJ software (National Institutes of Health; $n = 4$; *, $P < 0.05$). (D) Coimmunoprecipitation of NR2A subunit of NMDAR with the α7nAChR from solubilized rat brain tissue in various brain regions (top). Western blot analysis of the α7nAChR from various brain regions (bottom). Blots represent three independent experiments performed. IB, immunoblot; VTA, ventral tegmental area; Hippo, hippocampus; PFC, prefrontal cortex; STR, striatum; AMG, amygdala. (E) Effects of choline or choline/NMDA pretreatment of hippocampal primary cultures on the coimmunoprecipitation of NR2A with the α7nAChR. (F) Effects of chronic nicotine exposure on the α7nAChR–NR2A interaction in rat hippocampus. (G) Quantification of the α7nAChR–NR2A interaction with/without chronic nicotine treatment ($n = 3$; *, $P < 0.05$). Blots represent three independent experiments performed. (C and G) Error bars represent mean ± SEM.

hippocampal tissue. As depicted in Fig. 1 A (top), NR2A antibody was able to coimmunoprecipitate with α7nAChR from rat hippocampal homogenate, as recognized by a specific antibody for α7nAChR with an apparent relative molecular mass of 55,000 (M_r 55K). To rule out the possibility that the observed α7nAChR–NR2A interaction was caused by the nonspecificity of α7nAChR antibody, we performed a reverse coimmunoprecipitation. As shown in Fig. 1 A (bottom), α7nAChR antibody but not α4nAChR antibody can coimmunoprecipitate the NR2A subunit from rat hippocampal homogenate. These data suggested that α7nAChR and NMDAR may form a protein complex in the rat hippocampus. Furthermore, we measured the amount of NR2A coimmunoprecipitated by α7nAChR primary antibody versus total NR2A in the same amount of hippocampal protein used in the coimmunoprecipitation experiment. As shown in Fig. 1 (B and C), 53 ± 0.98% of NR2A forms a complex with α7nAChR in the rat hippocampus ($n = 4$; $P < 0.05$). We also examined whether α7nAChR forms a complex with NMDAR in other brain areas. As shown in Fig. 1 D (top), α7nAChR antibody was able to coimmunoprecipitate the NR2A subunit from protein extracted from the amygdala but failed to coimmunoprecipitate the NR2A subunit from proteins extracted from the striatum, prefrontal cortex, and ventral tegmental area. The expression of the NR2A and α7nAChR subunit in all of these areas was confirmed (Fig. 1 D, bottom). These results further validated the specificity of all the antibodies used in our coimmunoprecipitation experiments and confirmed the existence of the NR2A–α7nAChR interaction.

We then tested whether the α7nAChR–NR2A complex is involved in the actions of nicotine. We hypothesized that activation of the α7nAChR may alter α7nAChR–NR2A complex formation if α7nAChR–NR2A coupling participates in the molecular mechanisms of nicotine dependence. To investigate this possibility, we examined the ability of the NR2A antibody to coimmunoprecipitate with the α7nAChR in hippocampal primary cultures treated with 1 mM choline or 50 μM choline/NMDA. As shown in Fig. 1 E, activation of α7nAChR by choline led to a significant increase in the α7nAChR–NR2A interaction. The magnitude of this change was similar to that induced by NMDA/choline cotreatment, suggesting that the interaction was up-regulated upon α7nAChR activation. We then examined the effect of chronic nicotine exposure on α7nAChR–NR2A complex formation. Rats were pretreated with either nicotine or saline for 7 d (subdermal osmotic mini pump, 6 mg/kg nicotine/day). As shown in Fig. 1 (F and G), coimmunoprecipitation results indicated that α7nAChR–NR2A complex formation was

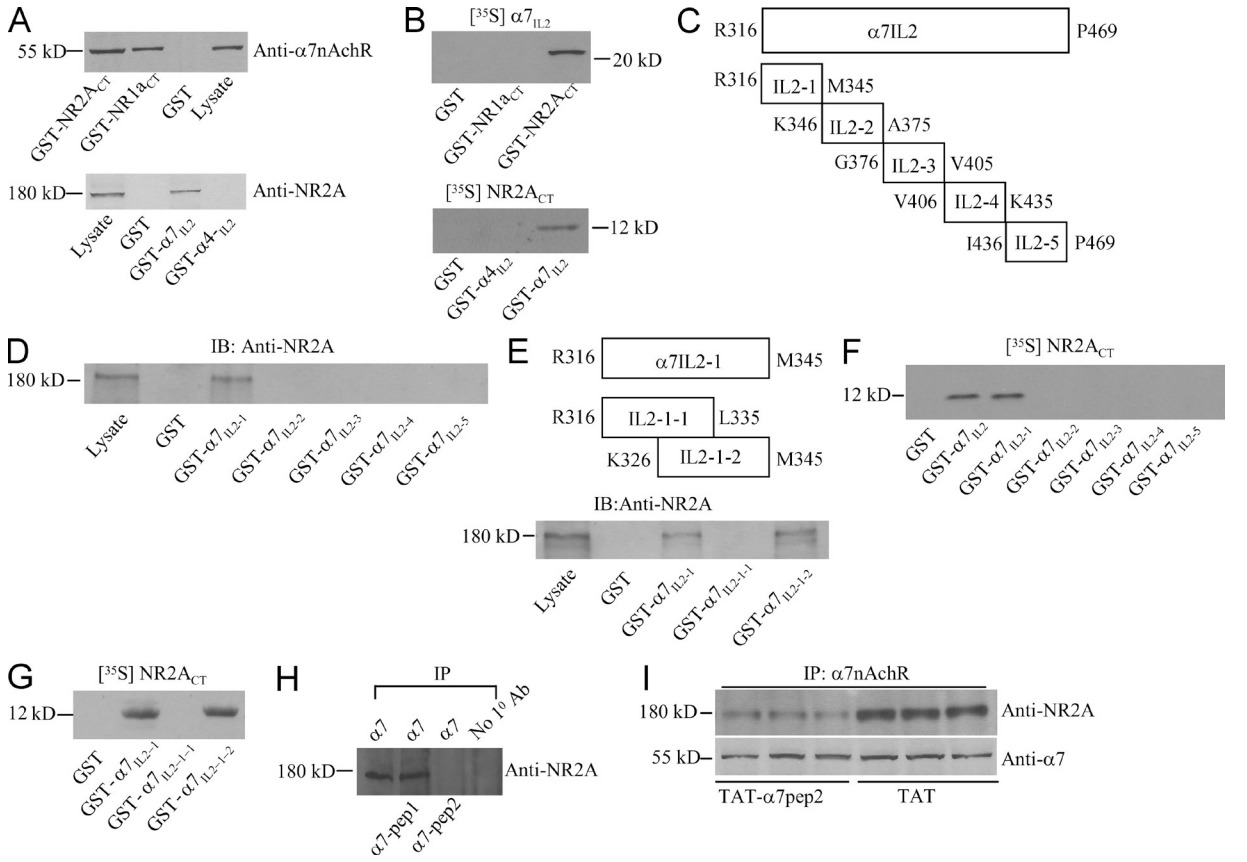

Figure 2. The NR2A subunit directly interacts with α7nAChR via the [L_{336}-M_{345}] region of α7nAChR. (A) Western blots of hippocampal α7nAChR, NR2A subunit of NMDAR (bottom) after affinity precipitation by GST-NR1a$_{CT}$, GST-NR2A$_{CT}$, and GST-α7$_{IL2}$ (R_{316}-P_{469}), respectively, but not GST-α4$_{IL2}$ or GST alone. (B) In vitro binding assay measuring direct binding of GST-NR2A$_{CT}$ to [^{35}S]α7$_{IL2}$ (top) and GST-α7$_{IL2}$ to [^{35}S]NR2A$_{CT}$ (bottom). (C) Schematic representation of the generated α7$_{IL2-1}$ to α7$_{IL2-5}$ fragments. (D) Western blot of hippocampal NR2A after affinity precipitation by the GST-α7$_{IL2-1}$: R_{316}-M_{345} fragment. (E) Schematic representation of the generated α7$_{IL2-1-1}$ and α7$_{IL2-1-2}$ fragments. Western blot of hippocampal NR2A after affinity precipitation by GST-α7$_{IL2-1-2}$: K_{326}-M_{345}. GST-α7$_{IL2-1}$ was used as a positive control (bottom). IB, immunoblot. (F) In vitro binding assay measuring direct binding of GST-α7$_{IL2-1}$ to [^{35}S]NR2A$_{CT}$. GST-α7$_{IL2}$ was used as a positive control. (G) In vitro binding assay measuring direct binding of GST-α7$_{IL2-1-2}$ to [^{35}S]NR2A$_{CT}$. GST-α7$_{IL2-1}$ was used as a positive control. (H) Association between NMDAR and α7nAChR upon the addition of α7pep2[L_{336}-M_{345}] peptide. (I) Protein–protein interaction between NMDAR and α7nAChR in the hippocampus. Coimmunoprecipitation (IP) of the NR2A subunit of NMDAR with α7nAChR from solubilized rat brain treated with TAT or TAT-α7pep2. Blots represent three independent experiments performed.

significantly enhanced in the hippocampus of rats chronically exposed to nicotine compared with animals treated with saline. These data implicate the formation of α7nAChR–NR2A complexes in the actions of nicotine.

We reasoned that if enhanced α7nAChR–NR2A coupling plays a role in the pathophysiology of nicotine dependence, disruption of α7nAChR–NR2A coupling might exert anti-addiction effects. To develop a protein peptide able to disrupt α7nAChR–NR2A coupling, we performed a series of biochemical analyses to identify the regions of the α7nAChR and NR2A that are essential for α7nAChR–NR2A complex formation. Both the carboxyl tail (CT) of the NR1/NR2A subunits and the second intracellular loop (IL2) of α7nAChR contain putative consensus sequences for receptor phosphorylation and potential binding sites for various proteins important in signaling (e.g., PSD-95, calmodulin, and Src kinase; Kornau et al., 1995; Ehlers et al., 1996; Wyszynski et al., 1997; Charpantier et al., 2005).To determine whether the CT regions of NR1a and NR2A subunits and the IL2 region of α7nAChR are involved in the formation of the α7nAChR–NMDAR complex, various glutathione *S*-transferase (GST) fusion proteins encoding the CT of the NR1a (GST-NR1a$_{CT}$: E_{834}-S_{938}) and NR2A (GST-NR2A$_{CT}$: D_{1350}-V_{1464}) subunits or the IL2 of the α7 (GST-α7$_{IL2}$: R_{316}-P_{469}) and α4 subunit of nAChR (GST-α4$_{IL2}$:V_{332}-K_{595}) were prepared and used in affinity purification assays. As shown in Fig. 2 A (top), both GST-NR1a$_{CT}$ and GST-NR2A$_{CT}$ but not GST alone precipitated solubilized hippocampal α7nAChR. Similarly, GST-α7$_{IL2}$ but not GST-α4$_{IL2}$ or GST alone precipitated solubilized hippocampal NR2A subunits (Fig. 2 A, bottom). Thus, α7nAChR and NMDAR can interact with each other through the IL2 of α7nAChR and the CT of NR1a and NR2A.

Although these results demonstrate the presence of the α7nACh–NMDA protein complex in rat hippocampal tissue, they do not show whether the α7nACh–NMDAR complex

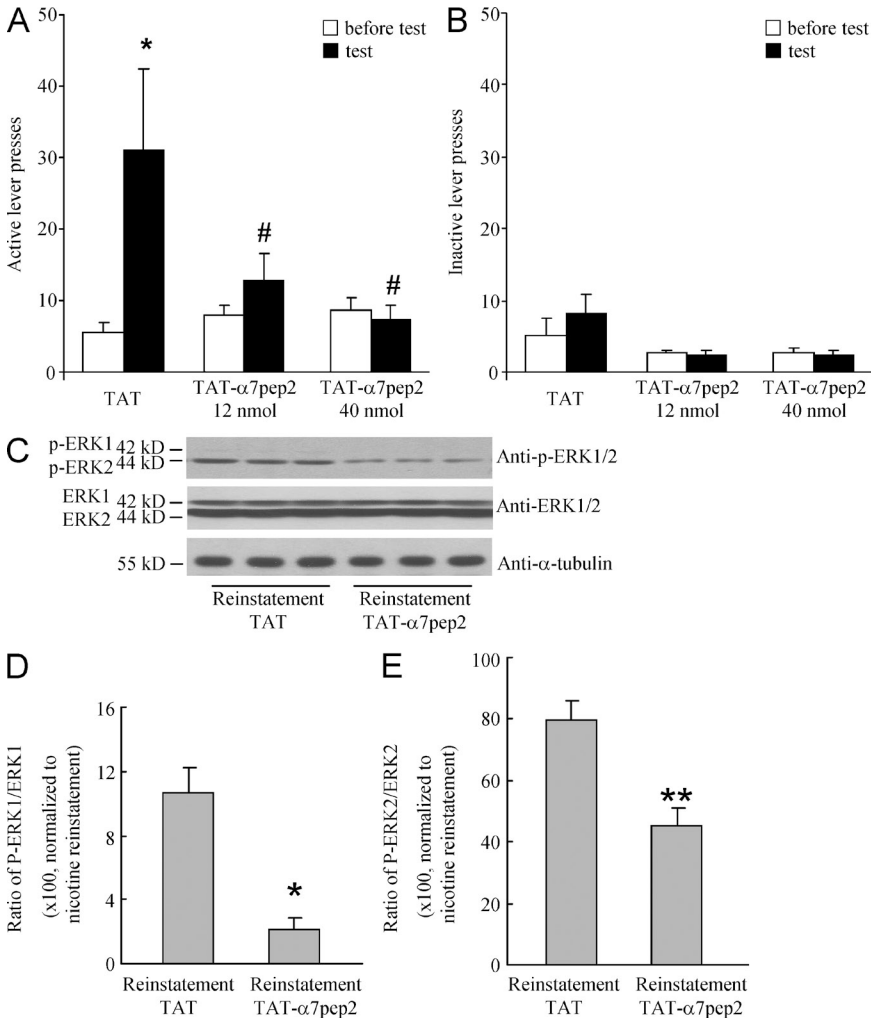

Figure 3. TAT-α7pep2 treatment blocks cue-induced reinstatement and ERK1/2 phosphorylation. (A and B) Active (A) and inactive (B) lever presses on the last day of extinction and on the test day for nicotine reinstatement. On the reinstatement test day, rats were tested in the presence of the response-contingent light + tone cue after injection with 40 nmol TAT or 12 and 40 nmol TAT-α7pep2[L_{336}-M_{345}] 1 h before testing. "#" indicates significant difference from control (TAT) on the test day ($P < 0.05$). (C) Western blot analysis of pERK1/2 and ERK1/2 in hippocampal proteins extracted from rats that reinstated nicotine seeking and were treated with 40 nmol TAT-α7pep2[L_{336}-M_{345}]. (D and E) Quantification of pERK1/ERK1 (D) and pERk2/ERK2 (E) in hippocampal proteins extracted from rats that reinstated nicotine seeking and were treated with 40 nmol TAT-α7pep2[L_{336}-M_{345}]. (A, B, D, and E) Error bars represent mean ± SEM (*, $P < 0.05$; **, $P < 0.01$; one-way ANOVA).

was formed through a direct interaction or indirectly via the involvement of an accessory binding protein. Using in vitro binding assays, we provide evidence that the α7nAChR and NR2A subunits interact directly. As shown in Fig. 2 B (top), an in vitro translated [^{35}S]$\alpha7_{IL2}$ probe hybridized with GST-$NR2A_{CT}$ but not GST-$NR1a_{CT}$ or GST alone, indicating that a direct protein–protein interaction can occur between the α7nAChR and the NR2A subunit, whereas the association between α7nAChR and NR1a subunits occurred most likely via an interaction between the NR1a and the NR2A subunits. Similarly, the [^{35}S]NR2A probe hybridized with GST-$\alpha7_{IL2}$ but not GST-$\alpha4_{IL2}$ or GST alone (Fig. 2 B, bottom), confirming the specificity of the direct protein–protein interaction between α7nACh and NR2A subunit of NMDAR.

To confirm these results and to delineate the region of the $\alpha7_{IL2}$ involved in the interaction with NR2A, five $\alpha7_{IL2}$ GST fusion proteins ($\alpha7_{IL2-1}$: R_{316}-M_{345}, $\alpha7_{IL2-2}$: K_{346}-A_{375}, $\alpha7_{IL2-3}$: G_{376}-V_{405}, $\alpha7_{IL2-4}$: V_{406}-K_{435}, and $\alpha7_{IL2-5}$: I_{436}-P_{469}) were constructed (Fig. 2 C) and used in affinity purification assays. As shown in Fig. 2 D, only GST-$\alpha7_{IL2-1}$ was able to precipitate NR2A, thus defining a discrete region of the α7nAChR that interacted with NR2A. Using a similar approach, $\alpha7_{IL2-1}$ was dissected into two smaller fragments, $\alpha7_{IL2-1-1}$: R_{316}-L_{335} and $\alpha7_{IL2-1-2}$: K_{326}-M_{345}, with a 10-aa (K_{326}-L_{335}) overlapping region to avoid the possible disruption of the binding motif (Fig. 2 E, top). Affinity purification assays identified $\alpha7_{IL2-1-2}$: K_{326}-M_{345} as the specific region of α7 that formed a protein complex with NR2A. As shown in Fig. 2 E (bottom), GST-$\alpha7_{IL2-1-2}$ was able to precipitate NR2A, whereas GST-$\alpha7_{IL2-1-1}$ and GST alone failed to precipitate NR2A from solubilized rat hippocampal tissue.

Consistent with the results of the affinity purification experiments, in vitro translated [^{35}S]$NR2A_{CT}$ probe hybridized only with GST-$\alpha7_{IL2-1}$ (Fig. 2 F) and GST-$\alpha7_{IL2-1-2}$ (Fig. 2 G). As GST-$\alpha7_{IL2-1-1}$ and GST-$\alpha7_{IL2-1-2}$ were designed with 10-aa (K_{326}-L_{335}) overlapping regions, the fact that only GST-$\alpha7_{IL2-1-2}$ interacted with the $NR2A_{CT}$ suggests that the L_{336}-M_{345} region of IL2 of α7nAChR is critical in the direct protein–protein interaction between α7nAChR and the NR2A subunit of NMDAR. This was further confirmed by the results of coimmunoprecipitation experiments. As shown in Fig. 2 H, preincubation with the synthetic peptide α7pep2[L_{336}-M_{345}] but not α7pep1[R_{316}-G_{325}] abolished the α7nACh–NR2A interaction, suggesting that α7pep2[L_{336}-M_{345}] is able to disrupt the α7nAChR–NR2A interaction.

We have shown that the α7nACh–NR2A interaction is up-regulated in brain tissue from rats chronically exposed to nicotine, and we have generated an interfering peptide that can disrupt the α7nACh–NR2A interaction. We then investigated whether disrupting the α7nACh–NR2A interaction would affect behaviors related to nicotine dependence. The ability of transactivator of transcription (TAT)–α7pep2[L_{336}-M_{345}] to disrupt α7nACh–NR2A interaction in vivo was confirmed by coimmunoprecipitation experiments. As shown in Fig. 2 I, TAT-α7pep2[L_{336}-M_{345}] (intracerebroventricular [ICV], 40 nmol) but not TAT alone significantly blocked the α7nAChR–NR2A interaction. We initially evaluated the effects of the interfering peptide on operant self-administration of nicotine. ICV injection of TAT-α7pep2[L_{336}-M_{345}] peptide had no effect on nicotine self-administration behaviors (not depicted). We then examined the effects of the α7pep2[L_{336}-M_{345}] peptide in a reinstatement procedure that is a validated animal model of relapse. As shown in Fig. 3 (A and B), re-exposure to cues previously associated with nicotine self-administration reinstated nicotine seeking, as indexed by increased responding on the active lever previously associated with nicotine delivery. ICV injection of 12 or 40 nmol TAT-α7pep2[L_{336}-M_{345}] blocked reinstatement of nicotine seeking.

To exclude the possibility that the inhibitory effect of the TAT-α7pep2[L_{336}-M_{345}] peptide is caused by a general suppression of behavior, we next tested whether or not TAT-α7pep2[L_{336}-M_{345}] peptide would affect locomotor activity. TAT-α7pep2[L_{336}-M_{345}] peptide did not affect locomotor activity (not depicted). The absence of effects on nicotine self-administration and general locomotor activity indicated that the attenuation of cue-induced reinstatement of these various reinforcers by TAT-α7pep2[L_{336}-M_{345}] did not appear to be caused by an impairment of motor function. Collectively, these results showed that TAT-α7pep2 had a specific effect on cue-induced nicotine reinstatement without affecting the general motor activity.

Accumulated evidence has demonstrated that extracellular signal-regulated kinase (ERK) activity is associated with drug reinstatement (Lu et al., 2005, 2006; Schroeder et al., 2008; Shiflett et al., 2008). To examine the potential downstream signaling that is involved in α7nACh–NMDAR protein complex formation, we measured ERK1/2 activation by Western blot analysis using anti–phospho-ERK antibody after reinstatement testing. As shown in Fig. 3 (C–E), TAT-α7pep2[L_{336}-M_{345}] peptide injection but not the TAT injection significantly reduced phospho-ERK1 and phosphor-ERK2 levels induced by a nicotine-associated cue, which also induced reinstatement. There was no significant change in the total ERK1 and ERK2 level. These data suggest that ERK signaling may be part of the downstream pathway associated with α7nACh–NMDAR protein complex formation.

In summary, our results provide the first direct evidence that two distinct ligand-gated ion channels can form a protein complex through a direct protein–protein interaction. Furthermore, we generated an interfering protein peptide, TAT-α7pep2[L_{336}-M_{345}], which can disrupt the formation of this α7nACh–NMDAR complex. Most importantly, we found that administration of this interfering peptide blocked cue-induced reinstatement of seeking. Our data not only provide the first evidence for a functional interaction between different ligand-gated ion channels through heterodimerization, but also point to a novel therapeutic target with direct implications for the treatment of relapse.

MATERIALS AND METHODS

Primary dissociated cell culture. Hippocampus was collected from fetal (embryonic day 18) Wistar rats. Pregnant rats were anesthetized by inhalation of halothane or isoflurane and killed by cervical dislocation, and were fetuses removed. The dissection and dissociation were performed in ice-cold HBSS (without Ca^{2+} and Mg^{2+}; Gibco) supplemented with 10 mM Hepes, pH 7.4, and 1 mM sodium pyruvate. Neurons were mechanically dispersed by trituration using glass Pasteur pipettes with reduced tips and then added to plating solution composed of 89.5% Neurobasal (Gibco), 10% horse serum, 0.5% penicillin/streptomycin (P/S). The cells were plated on glass coverslips coated with 0.1 mg/ml poly-D-lysine in borate buffer. The cell density was ∼50,000–80,000/ml. After 5/6 h of plating, half of the plating solution was replaced by feeding solution containing 98% Neurobasal, 2% B-27 supplement, 0.5 mM L-glutamine, and 0.5% P/S (all from Gibco). Twice per week, half of the solution was replaced with fresh feeding solution. After 6 d of plating, 5 μM Ara-C was added to stop the growth of glial cells.

GST fusion proteins. To construct GST fusion proteins encoding fragments of NR1, NR2A, α4nAChR, and α7nAChR subunits, cDNA fragments were amplified by PCR with specific primers. Except where specified, all 5′ and 3′ oligonucleotides incorporated BamH1 (GGATCC) and Xho1 sites (CTCGAG), respectively, to facilitate subcloning into the pGEX-4T3 vector. GST fusion proteins were prepared from bacterial lysates as described by the manufacturer (GE Healthcare). To confirm appropriate splice fusion and the absence of PCR-generated nucleotide errors, all constructs were sequenced.

Protein affinity purification, in vitro binding, coimmunoprecipitation, and Western blot. Coimmunoprecipitation, affinity pull-down, and Western blot analyses were performed as previously described (Liu et al., 2000; Lee et al., 2002; Pei et al., 2010). For coimmunoprecipitation experiments, solubilized rat hippocampal extracts (500∼700 μg protein) were incubated in the presence of specific primary antibodies anti-NR2A (EMD Millipore), anti-α4 (EMD Millipore), anti-α7 (Santa Cruz Biotechnology, Inc.), or 1∼2 μg control IgG for 4 h at 4°C, followed by the addition of 20 μl protein A/G agarose (Santa Cruz Biotechnology, Inc.) for 12 h. Pellets were washed, boiled for 5 min in SDS sample buffer, and subjected to SDS-PAGE. 20∼50 μg of extracted protein was used as control in each experiment. For affinity purification experiments, solubilized hippocampal extracts (50–100 μg protein) were incubated with glutathione–Sepharose beads (GE Healthcare) bound to 50∼100 μg GST fusion proteins at room temperature for 1 h. Beads were washed, boiled for 5 min in SDS sample buffer, and subjected to SDS-PAGE. After transfer of proteins onto nitrocellulose, membranes were Western blotted with polyclonal α4 antibody (EMD Millipore), polyclonal α7 antibody (Santa Cruz Biotechnology, Inc.), α-tubulin (Sigma-Aldrich), Phospho-Erk1/2 and Erk1/2 (Cell Signaling Technology), or monoclonal NR2A antibody (BD). For in vitro binding experiments, glutathione beads carrying 20 μg GST fusion proteins were incubated at room temperature for 1 h with [^{35}S]methionine-labeled probes. The beads were then washed six times with PBS containing 0.1–0.5% (vol/vol) Triton X-100 and eluted with 10 mM glutathione elution buffer. Eluates were separated by SDS-PAGE and visualized by autoradiography using BioMax (Kodak) film.

TAT-conjugated peptides. The α7-pep1 and α7-pep2 peptides were rendered cell permanent by fusing each to the cell membrane transduction domain of the HIV-1 TAT protein (Tyr-Gly-Arg-Lys-Lys-Arg-Arg-Gln-Arg-Arg-Arg).

Implantation of osmotic mini pumps. Adult male Long-Evans rats (Charles River) weighing 250–275 g were surgically implanted with subcutaneous osmotic mini pumps (C type 2001; Alzet Osmotic Pumps) designed to deliver a continuous infusion of nicotine for 7 d according to methods described previously (Shram et al., 2008). To implant the mini pumps, rats were anesthetized with isoflurane, and then a small incision was made between the shaved scapulae and the pump was inserted under the skin, which was then sutured. Rats in the nicotine treatment groups were implanted with pumps set to deliver nicotine at a dose of 6 mg/kg/day nicotine (in base form) for 7 d. Control rats were implanted with a sham pump.

Nicotine self-administration and reinstatement of nicotine seeking. Male Long-Evans rats underwent training for operant responding for 45-mg sucrose pellets for 3 d. They were then implanted with catheters into the right jugular vein under general anesthesia (75 mg/kg ketamine/10 mg/kg xylazine, i.p.) according to methods described previously (Corrigall and Coen, 1989; Lê et al., 2006; Shram et al., 2008). After recovery from surgery, rats were trained to self-administer nicotine in operant chambers (Med Associates). Each chamber was equipped with two levers located 2.5 cm above the floor. Depressing the active lever activated a high speed microliter syringe pump (PHM-104; Med Associates). Pressing the inactive lever was recorded but had no programmed consequences. A white cue light was positioned above the active lever, and a tone generator (2,900 Hz) was located directly above the cue light; both visual (40 s) and auditory (1 s) stimuli were turned on when a nicotine reinforcement was obtained. A modified 22-gauge cannula was attached to the i.v. catheter on a daily basis, and this was connected to a fluid swivel with Tygon tubing protected by a metal spring. The swivel was attached to syringe containing nicotine solution with Tygon tubing.

Rats initiated self-administration of nicotine (0.03 mg/kg/infusion) under an FR-1 schedule for five daily 1-h sessions. Time out after nicotine infusion was 40 s, and during this time, pressing on the active lever had no programmed consequences but was recorded. Rats were then placed on FR-2 and FR-3 schedules for three and four sessions each, respectively. They were then implanted with ICV cannulae (as described in the next section) for subsequent injection of the peptide. Nicotine self-administration was then restabilized for 3 d at FR-3 schedule after recovery from surgery. The effects of TAT-α7pep2 (TAT, TAT-α7-pep2: 12 or 40 nmol in 4 µl vehicle) on nicotine self-administration were examined in 12 rats that achieved stable nicotine self-administration in a Latin square design. The peptide was infused ICV over 60 s, and the injector remained in place for an additional 60 s, 1 h before self-administration testing.

To evaluate the effects of peptide on reinstatement of nicotine seeking, a separate group of rats ($n = 12$) trained to self-administer nicotine was used. Extinction of their nicotine self-administration was performed until the rats pressed on the active lever <15 times during a 1-h session. Extinction sessions (14 sessions, 1 session per day) were performed in the same manner as those described for the self-administration with the exception that pressing on the lever did not deliver nicotine nor did it activate light + tone cues previously paired with nicotine delivery.

The effects of TAT-α7pep2 (TAT, TAT-α7-pep2: 12 or 40 nmol in 4 µl vehicle) on reinstatement of nicotine seeking induced by reexposure to the light + tone cue were examined in a Latin square design. The peptide was infused ICV over 60 s, and the injector remained in place for an additional 60 s, 1 h before reinstatement testing. For reinstatement testing, a light + tone cue without delivery of nicotine marked the beginning of the session, and for the remainder of the session the cues were delivered on an FR-3 schedule, as during self-administration. A minimum of two daily extinction sessions occurred between test days.

ICV cannulation surgery and microinjection. Surgery was performed under ketamine/xylazine anesthesia as described in the previous section. Using standard stereotaxic techniques, 23-gauge stainless steel guide cannulae (Plastics One) were implanted into the right lateral ventricle 1 mm over the target region and affixed to the skull by dental acrylic and jeweler screws. The final coordinates for the injector tip (from Bregma) are as follows: AP −1 mm, LM 1.4 mm, and DV −3.7 mm from the dura. ICV infusions were administered by a 10-µl syringe connected via polyethylene tubing to a 30-gauge injector that extended 1 mm below the tip of the guide cannula. At the end of the experiment, cannula patency was confirmed with an ICV injection of 50 ng angiotensin and by observing subsequent water drinking behavior. Placements were considered accurate if a rat started to drink within 1 min of the infusion and sustained drinking over 2 min. Three rats were eliminated from the analysis of the data as the result of blocked i.v. or ICV cannulae (two) or because they did not reach extinction criterion.

Locomotor testing. After recovery from surgery, rats were habituated to the locomotor activity boxes daily for 1-h sessions for 4 d. Horizontal activity was measured by the number of infrared beam breaks over this period. After the habituation period, rats were pretreated with peptide or scrambled control peptide, and effects on locomotor activity were recorded for 1 h.

Data analysis. Data are presented as mean ± SEM. For the neurochemical data, one-way ANOVAs were used, with planned comparisons for post hoc analyses. For reinstatement experiments, total lever pressing was analyzed with mixed ANOVAs using appropriate between- and within-subject factors. Significance was set at $\alpha = 0.05$.

The work is supported by the Centre for Addiction and Mental Health (F. Liu), Canadian Institutes of Health Research (F. Liu), and BioDiscovery Toronto (F. Liu).

The authors declare no competing financial interests.

Submitted: 14 June 2012
Accepted: 17 September 2012

REFERENCES

Aramakis, V.B., and R. Metherate. 1998. Nicotine selectively enhances NMDA receptor-mediated synaptic transmission during postnatal development in sensory neocortex. *J. Neurosci.* 18:8485–8495.

Bulenger, S., S. Marullo, and M. Bouvier. 2005. Emerging role of homo- and heterodimerization in G-protein-coupled receptor biosynthesis and maturation. *Trends Pharmacol. Sci.* 26:131–137. http://dx.doi.org/10.1016/j.tips.2005.01.004

Charpantier, E., A. Wiesner, K.H. Huh, R. Ogier, J.C. Hoda, G. Allaman, M. Raggenbass, D. Feuerbach, D. Bertrand, and C. Fuhrer. 2005. Alpha7 neuronal nicotinic acetylcholine receptors are negatively regulated by tyrosine phosphorylation and Src-family kinases. *J. Neurosci.* 25:9836–9849. http://dx.doi.org/10.1523/JNEUROSCI.3497-05.2005

Corrigall, W.A., and K.M. Coen. 1989. Nicotine maintains robust self-administration in rats on a limited-access schedule. *Psychopharmacology (Berl.).* 99:473–478. http://dx.doi.org/10.1007/BF00589894

Ehlers, M.D., S. Zhang, J.P. Bernhadt, and R.L. Huganir. 1996. Inactivation of NMDA receptors by direct interaction of calmodulin with the NR1 subunit. *Cell.* 84:745–755. http://dx.doi.org/10.1016/S0092-8674(00)81052-1

Epstein, D.H., K.L. Preston, J. Stewart, and Y. Shaham. 2006. Toward a model of drug relapse: an assessment of the validity of the reinstatement procedure. *Psychopharmacology (Berl.).* 189:1–16. http://dx.doi.org/10.1007/s00213-006-0529-6

Fisher, J.L., and J.A. Dani. 2000. Nicotinic receptors on hippocampal cultures can increase synaptic glutamate currents while decreasing the NMDA-receptor component. *Neuropharmacology.* 39:2756–2769. http://dx.doi.org/10.1016/S0028-3908(00)00102-7

Gray, R., A.S. Rajan, K.A. Radcliffe, M. Yakehiro, and J.A. Dani. 1996. Hippocampal synaptic transmission enhanced by low concentrations of nicotine. *Nature.* 383:713–716. http://dx.doi.org/10.1038/383713a0

Kenny, P.J., E. Chartoff, M. Roberto, W.A. Carlezon Jr., and A. Markou. 2009. NMDA receptors regulate nicotine-enhanced brain reward function and intravenous nicotine self-administration: role of the ventral tegmental

area and central nucleus of the amygdala. *Neuropsychopharmacology*. 34: 266–281. http://dx.doi.org/10.1038/npp.2008.58

Kim, E., and M. Sheng. 2004. PDZ domain proteins of synapses. *Nat. Rev. Neurosci*. 5:771–781. http://dx.doi.org/10.1038/nrn1517

Kornau, H.C., L.T. Schenker, M.B. Kennedy, and P.H. Seeburg. 1995. Domain interaction between NMDA receptor subunits and the postsynaptic density protein PSD-95. *Science*. 269:1737–1740. http://dx.doi.org/10.1126/science.7569905

Lê, A.D., Z. Li, D. Funk, M. Shram, T.K. Li, and Y. Shaham. 2006. Increased vulnerability to nicotine self-administration and relapse in alcohol-naive offspring of rats selectively bred for high alcohol intake. *J. Neurosci*. 26:1872–1879. http://dx.doi.org/10.1523/JNEUROSCI.4895-05.2006

Lee, F.J., S. Xue, L. Pei, B. Vukusic, N. Chéry, Y. Wang, Y.T. Wang, H.B. Niznik, X.M. Yu, and F. Liu. 2002. Dual regulation of NMDA receptor functions by direct protein-protein interactions with the dopamine D1 receptor. *Cell*. 111:219–230. http://dx.doi.org/10.1016/S0092-8674(02)00962-5

Lee, S.P., Z. Xie, G. Varghese, T. Nguyen, B.F. O'Dowd, and S.R. George. 2000. Oligomerization of dopamine and serotonin receptors. *Neuropsychopharmacology*. 23:S32–S40. http://dx.doi.org/10.1016/S0893-133X(00)00155-X

Levitan, I.B. 1994. Modulation of ion channels by protein phosphorylation and dephosphorylation. *Annu. Rev. Physiol*. 56:193–212. http://dx.doi.org/10.1146/annurev.ph.56.030194.001205

Liu, F., Q. Wan, Z.B. Pristupa, X.M. Yu, Y.T. Wang, and H.B. Niznik. 2000. Direct protein-protein coupling enables cross-talk between dopamine D5 and gamma-aminobutyric acid A receptors. *Nature*. 403:274–280. http://dx.doi.org/10.1038/35001232

Lu, L., B.T. Hope, J. Dempsey, S.Y. Liu, J.M. Bossert, and Y. Shaham. 2005. Central amygdala ERK signaling pathway is critical to incubation of cocaine craving. *Nat. Neurosci*. 8:212–219. http://dx.doi.org/10.1038/nn1383

Lu, L., E. Koya, H. Zhai, B.T. Hope, and Y. Shaham. 2006. Role of ERK in cocaine addiction. *Trends Neurosci*. 29:695–703. http://dx.doi.org/10.1016/j.tins.2006.10.005

MacDermott, A.B., M.L. Mayer, G.L. Westbrook, S.J. Smith, and J.L. Barker. 1986. NMDA-receptor activation increases cytoplasmic calcium concentration in cultured spinal cord neurones. *Nature*. 321:519–522. http://dx.doi.org/10.1038/321519a0

Milligan, G., and N.J. Smith. 2007. Allosteric modulation of heterodimeric G-protein-coupled receptors. *Trends Pharmacol. Sci*. 28:615–620. http://dx.doi.org/10.1016/j.tips.2007.11.001

Pei, L., S. Li, M. Wang, M. Diwan, H. Anisman, P.J. Fletcher, J.N. Nobrega, and F. Liu. 2010. Uncoupling the dopamine D1-D2 receptor complex exerts antidepressant-like effects. *Nat. Med*. 16:1393–1395. http://dx.doi.org/10.1038/nm.2263

Prendergast, M.A., B.R. Harris, S. Mayer, R.C. Holley, J.R. Pauly, and J.M. Littleton. 2001. Nicotine exposure reduces N-methyl-D-aspartate toxicity in the hippocampus: relation to distribution of the alpha7 nicotinic acetylcholine receptor subunit. *Med. Sci. Monit*. 7:1153–1160.

Schroeder, J.P., M. Spanos, J.R. Stevenson, J. Besheer, M. Salling, and C.W. Hodge. 2008. Cue-induced reinstatement of alcohol-seeking behavior is associated with increased ERK1/2 phosphorylation in specific limbic brain regions: blockade by the mGluR5 antagonist MPEP. *Neuropharmacology*. 55:546–554. http://dx.doi.org/10.1016/j.neuropharm.2008.06.057

Sheng, M. 2001. Molecular organization of the postsynaptic specialization. *Proc. Natl. Acad. Sci. USA*. 98:7058–7061. http://dx.doi.org/10.1073/pnas.111146298

Shiflett, M.W., R.P. Martini, J.C. Mauna, R.L. Foster, E. Peet, and E. Thiels. 2008. Cue-elicited reward-seeking requires extracellular signal-regulated kinase activation in the nucleus accumbens. *J. Neurosci*. 28:1434–1443. http://dx.doi.org/10.1523/JNEUROSCI.2383-07.2008

Shram, M.J., E.C. Siu, Z. Li, R.F. Tyndale, and A.D. Lê. 2008. Interactions between age and the aversive effects of nicotine withdrawal under mecamylamine-precipitated and spontaneous conditions in male Wistar rats. *Psychopharmacology (Berl.)*. 198:181–190. http://dx.doi.org/10.1007/s00213-008-1115-x

Smart, T.G. 1997. Regulation of excitatory and inhibitory neurotransmitter-gated ion channels by protein phosphorylation. *Curr. Opin. Neurobiol*. 7:358–367. http://dx.doi.org/10.1016/S0959-4388(97)80063-3

Swope, S.L., S.J. Moss, L.A. Raymond, and R.L. Huganir. 1999. Regulation of ligand-gated ion channels by protein phosphorylation. *Adv. Second Messenger Phosphoprotein Res*. 33:49–78. http://dx.doi.org/10.1016/S1040-7952(99)80005-6

Wyszynski, M., J. Lin, A. Rao, E. Nigh, A.H. Beggs, A.M. Craig, and M. Sheng. 1997. Competitive binding of alpha-actinin and calmodulin to the NMDA receptor. *Nature*. 385:439–442. http://dx.doi.org/10.1038/385439a0